Int J Adv Manuf Technol (2018) 94:3819–3828
DOI 10.1007/s00170-017-1058-7

ORIGINAL ARTICLE

A metal additive manufacturing method: semi-solid metal extrusion and deposition

Amin Jabbari[1] · **Karen Abrinia**[1]

Received: 20 April 2017 / Accepted: 11 September 2017 / Published online: 25 September 2017

Abstract Different existing metal additive manufacturing (AM) processes have many shortcomings and a lot of activities are centered on improving the final printed metal product. A new method of metal additive manufacturing has been proposed in this paper. Unlike most of the metal additive manufacturing processes, it does not use metal powder. The proposed method utilizes semi-solid metal (SSM) forming combined with deposition process as used in the most common additive manufacturing process for polymers. SSM forming is a promising near net shape technology with several advantages, such as being a porosity-free product and having reduced shrinkage, controlled microstructure, and excellent mechanical performance. Implementation of this technology in metallic additive manufacturing improves the mechanical properties and cost savings. Complicated time-dependent behavior of SSM makes it a challenging issue to utilize in additive manufacturing. A wire feedstock as a metallic filament was employed for the proposed process. However, some material preparations were necessary to get the desired rheological properties at the deposition head. In this study, the strain-induced melt-activated (SIMA) process was applied on a low-melting-temperature Sn-Pb alloy to obtain the desired globular feedstock microstructure. Then, preconditioned wire was fed in a thixo-extruder, which was designed and built for the proposed method in this research. A semi-melted alloy was deposited on the moving substrate to build a metallic part layer by layer. Various parameters of SIMA and thixo-extrusion processes, including wire thermomechanical cycle, feed rate, solid fraction, nozzle and chamber geometry, and others, were examined experimentally, and a sustainable semi-solid metal extrusion and deposition (SSMED) process was achieved. Finally, an acceptable metallurgical layer bonding was obtained at the interface of the deposited layers, with good mechanical properties of the fabricated parts. The new proposed method seems to have great potentials for metal additive manufacturing parts.

Keywords 3D printing · Semi-solid alloy · Wire thixo-extruder · Metallic filament

1 Introduction

Additive manufacturing is a technology that aims to reduce part costs by decreasing the material wastage and time to market [1]. It is one of the most growing and developing technologies in the recent years. The process includes layer-based manufacturing where the material is added in a layer-by-layer fashion to build the required product. AM could present better flexibility in geometry and great potential savings in time and cost [2]. There exist many different methods for this type of manufacturing for various materials such as polymers, ceramics, metals, and composites [3–8].

Complex industrial parts could be manufactured directly from CAD data using metallic additive manufacturing (AM). Up to date, there are three primary feedstock process forms for metal AM: (a) powder-bed methods, (b) powder-fed methods, (c) wire-fed methods; the first two uses laser or electron beam energy source for sintering/melting of the metal powder and the last one uses the same sources to melt a wire [6].

✉ Karen Abrinia
cabrinia@ut.ac.ir

Amin Jabbari
a.jabbari@ut.ac.ir

[1] School of Mechanical Engineering, College of Engineering, University of Tehran, Tehran, Iran

Powder-based methods have been successfully used to directly fabricate metallic parts by scanning an energy source over a powder bed of metal. While these methods are capable of creating near fully dense parts with a small feature size [9], but they have many inherent limitations. Some typical examples for these limitations are high costs, low deposition rates, high energy consumption, residual stresses, large thermal gradients, overall poor surface finish, limited part size, and high contamination risk due to big surface-to-weight ratio of the powder [10].

Wire feedstock method offers some advantages as regards the supply of material for metal AM. Due to simpler process setup and operation, wire-fed methods seem to offer better repeatability and higher deposition rates in contrast to powder [11]. To date, wire-fed AM utilizes three different energy sources of laser, arc welding, or electron beam [12]. Metal wires are lower in cost and more available than AM metal powders, making wire-fed processes more cost-effective and competitive. Moreover, it is a more environmentally friendly process, which does not expose operators to the powder hazards [12].

However, so far, all metal wire-fed AM use high-energy source to melt the wire and increase the temperature hundreds of degrees above the melting point of the alloy [8, 13]. In fact, these methods are very similar to automated welding processes and high temperature of the melt pool and intense thermal gradients around it are inevitable [14]. This leads to more controlled processing and post-processing operations to manipulate the microstructure and improve mechanical properties [15].

Developing a route that uses wire without most of the limitations described above is a great step to build structural metallic components by AM. High mechanical properties of semi-solid metal formed parts besides desired rheological properties in low processing temperatures, below liquidus line [16], exhorted the authors to utilize semi-solid metals (SSMs) for the AM process. It is known that extrusion-based processes are among the most widely used AM technologies and this is due to unparalleled advantages of these processes [17]. The feasibility of utilizing semi-solid metal extrusion and depositioning for the additive manufacturing of low-temperature metallic parts was confirmed in the work of Rice et al. [18]. Confirmation of process feasibility for use of metals extrusion paves the way for more detailed studies towards the development of a sustainable process.

Semi-solid metal extrusion and deposition (SSMED) allows for the formation of a metal stream with controllable rheology in a temperature range intermediate to that of liquid and solid processing. In addition, it allows for greater cleanliness and material integrity than fully melted processes and powder sintering. High productivity and lower energy consumption are goals for SSMED. The development of a combined SSM and AM technology by making semi-solid metal slurry input to an AM process will allow for significant reduction in costs and time for the production of viable large metallic prototypes and parts. Therefore, it is also in line with the low-cost objective in this work.

The main idea comes from additive manufacturing of polymers by fused deposition modeling (FDM) method. However, there are many obvious substantial differences between metallic alloys and commercial 3D printing polymeric materials. The main difference is in the rheological behavior of semi-melted polymers and metal alloys. In both cases, the material flows like a shear-thinning non-Newtonian fluid but the behavior is very different in details. Low glass transition and cold crystallization temperature of the polymers helps the plasticizing of the filament in a wide range of operating temperatures and the ease of extruding through the nozzle [19]. In the case of metallic alloys, they need to be processed in a narrow range of temperatures in which the alloy is in two-phase region (L+α) of the phase diagram with a desirable morphology and solid fraction [20]. Rice et al. [18] studied solid freeform fabrication of a metallic alloy via rheoforming route and partially solidifying the alloy. They used an electrical furnace to melt the alloy and a rheomolder to prepare in situ semi-solid slurry. This apparatus was massive and hard to move, and so the bed did all the movements. Furthermore, the deposited bead diameter was more than 3.5 mm and this was undesirable for the production of most of the industrial parts [21]. All of these shortcomings guided the authors to focus on thixo-extrusion process, which does not involve the molten metals and high energy consumption associated with it [22]. In the literature, some attempts have been sited to print the low-melting-temperature alloys in fully melted state [23–26]. A completely molten alloy has a very low viscosity causing turbulent flow of material which results in uncontrollable material flow and microstructure [27].

2 Experimental procedure

A basic AM apparatus consists of a combination of motion systems, feedstock, and the heat source [19]. The motion system used in this research was a Cartesian robot-like FDM machine. The concept of heat source and feedstock used here had also similarities to previous systems. However, a new head for thixo-extrusion of metallic filaments was developed and mounted on a carriage of a three-axis table. Nevertheless, the first step to additive manufacturing of semi-solid metals in this work was to prepare feedstock with suitable microstructure for thixo-extrusion. One of the key issues in SSM processing is breaking the as cast dendritic microstructure of raw material to a globular microstructure to improve rheological properties and printability [28]. There are several methods to obtain SSM desirable microstructure, which divide into two main categories: (a) rheoforming and (b) thixoforming. The

former refers to developing the semi-solid slurry from the molten metal whereas the latter utilizes a pretreated material with a non-dendritic microstructure [29] and is the one used in here.

2.1 Casting of alloys

The commercial pure Sn and Pb with > 99.5% purity were used and melted to form Sn–15%Pb and Pb–40%Sn alloys. The raw billets were casted in a cylindrical permanent die to build the starting material of the subsequent process to obtain a preconditioned wire with appropriate microstructure.

2.2 SIMA process

The main solid-state route to globular starting material was the strain-induced melt-activated (SIMA) process [30]. The material was deformed by extrusion and then heated and held in the semi-solid state. The liquid was formed around the fine and equiaxed grains along with its recrystallization. A fine and globular structure was a result of high-angle grain boundaries induced by plastic deformation and recrystallization wetted by liquid metal at the semi-solid temperature [29] (Fig. 1). The SIMA process was effective for small diameter feedstock and produced high quality feedstock for thixo-extrusion which also has the potential application for wrought alloys and high melting temperature alloys such as titanium and super alloys [20].

The as cast billets were extruded in a single-step cylindrical extrusion die set to reduce the diameter and produce the wire or filament which was supposed to be used as the feedstock for the thixo-extruding process. The extrusion ratio was about 70 at ambient temperature. Billets of 25 mm diameter were extruded to 3-mm-diameter wires with a 100-Ton hydraulic press. The extruded wire was warmed up to 40 °C due to large plastic deformation of 98% reduction in area. The ram speed was set at 4 mm/min to avoid extra heat generation. The extrusion die set, deformation zone, and produced wire are illustrated in Fig. 2.

To accomplish the SIMA thermomechanical procedure, the extruded wires were isothermally held in a semi-solid state to create round solid particles surrounded by liquid. This process was done in different solid fractions of 0.7, 0.5, and 0.4 and held for periods of 10, 15, and 20 min in a Memmert universal heating oven. Then, the wires were promptly quenched into cold water. The filaments were supported in a 3-mm Teflon tube and placed in the oven sinks horizontally. The resultant microstructures were studied and the best holding time and temperature values were investigated in order to obtain globular grains.

2.3 Design of filament thixo-extruder

To introduce the most affordable system, a desktop machine based on Prusa i3 FDM was assembled, which is said to be the most used 3D printer in the world [31]. Instead of the FDM printing head, a thixo-extruder was designed and built which used a metallic wire as a filament and deposited a uniform bead of semi-solid slurry on a bed to manufacture a metallic part layer by layer. At the entrance, the metallic filament was fed to hot end of the thixo-extruder via a pinch roller, and the solid portion of the filament acting as a piston to push the semi-molten alloy through a print nozzle. From physics of the problem, the most common failure mode of the filament feedstock in the FDM process was buckling [32]. The critical load (F_{cr}) could be calculated from the Euler's column formula for pin-ended boundary conditions (Eq. 1).

$$F_{cr} = \frac{\pi^3 E d_f^4}{64 L_f^2} \tag{1}$$

where E, d_f, and L_f are elastic modulus, filament diameter, and length, respectively. It is necessary to determine this load in the design of the wire feeder. Melting front was located in an intermediate point between the nozzle tip and the entrance of the filament where the filament temperature exactly reached solidus temperature of the alloy, which was 183 °C [33].

Due to economic considerations, in the newly designed thixo-extruder, it was tried to keep maximum similarity to commercial FDM hot ends. However, more complex rheology and sensitivity of SSMs to temperature variations made it necessary to try different designs. The best design evolved

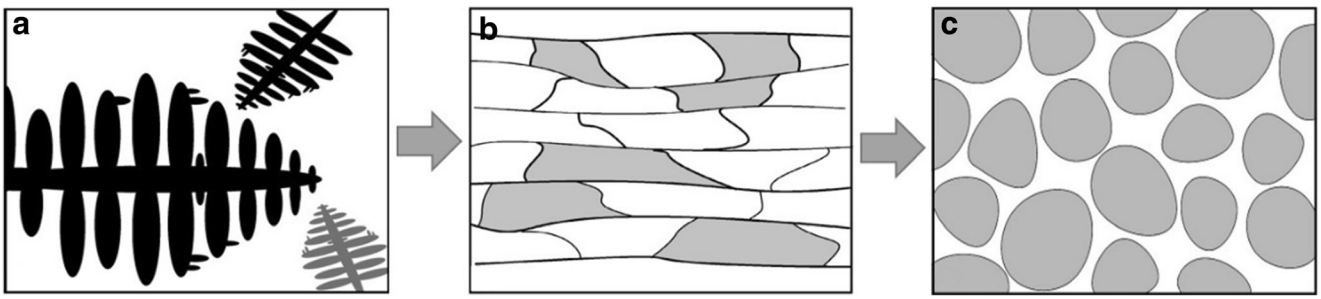

Fig. 1 Schematic of microstructure evolution during SIMA process. (a) Dendritic as cast, (b) directional after extrusion, and (c) globular after holding in semi-solid temperature

Fig. 2 The extrusion die set (left), deformation zone (up right), and produced wire (down right)

as shown in Fig. 3. Finally, in order to evenly distribute heat all around the sides of the liquefier chamber, a 60-W nozzle heater element was used surrounding the cylindrical hot end block. The amount of slurry in the liquefier would depend on the heat flux and the filament feed rate, and this was the critical design criteria for the thixo-extruder [34].

The heat barrier, made of stainless steel, was considered a good solution acting as the main physical limit to prevent heat conduction towards the upper part of the thixo-extruder. An annular heat sink was also designed and built above the heat barrier to minimize the heat conduction towards the cold end and feeder mechanism. The heat sink material was made of aluminum alloy just like liquefier to have maximum heat exchange.

2.4 SSMED experimental parameters

The main practical parameters that affect the experimental procedure of SSMED could be classified into four categories of liquefier geometrical parameters, feeding/moving speeds, temperature issues, and surface properties. Key elements of a SSMED process includes the feeding mechanism, liquefier dynamics, bead spreading, bonding of adjacent beads of alloys to one another, and shape changes due to thermal gradients within the part.

The thixo-extrusion experiments were carried out for both of the investigated alloys with increasing feed rates through nozzles with various sizes at different temperatures as shown in Table 1.

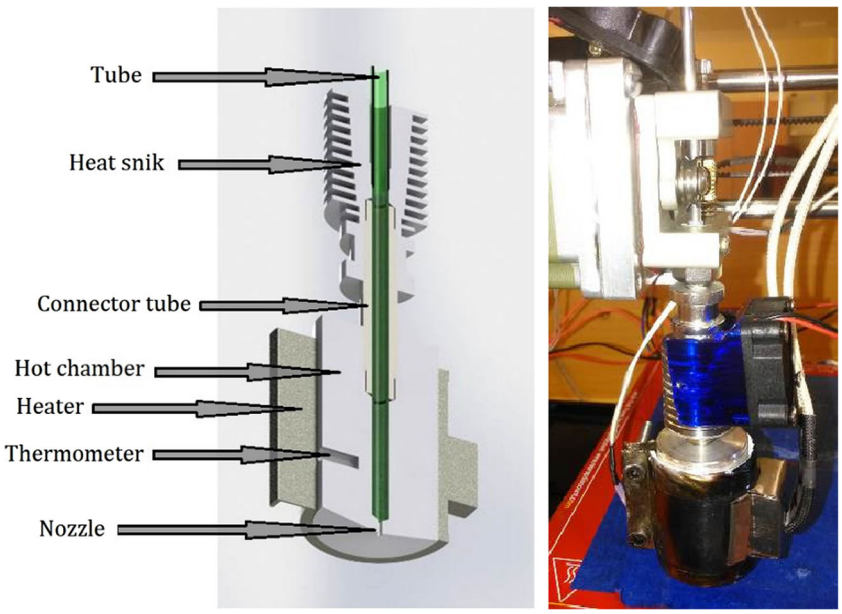

Fig. 3 Developed SSMED thixo-extruder

Table 1 The main experimental parameters in SSMED

Parameter	Feed rate	Solid fraction	Nozzle size	Channel length	Wall material
Amount	1–10 mm/s	0.3–0.5	1.5–2 mm	10–40 mm	Teflon-Al alloy-stainless steel

Distance between the orifice and the substrate was set to 1.1× the nozzle diameter. In practice, lower values cause smearing of the leaving material and more seriously cause a lesser control of the printing quality. The SIMA processed globular filament feeding to the hot end was warmed up to semi-solid temperature and simultaneously thixo-extruded through the nozzle to deposit on the surface or lower layer. In situ isothermal holding times of filaments during SSMED process were in the range of 4–40 s for the investigated feed rates.

Due to inherent differences of rheological properties of commercial FDM materials with semi-solid alloys, 3D printer firmware was modified to accommodate changes in the control of axes movements, temperature PID control, and extruder motor settings. These necessary modifications were done on Marlin firmware at Arduino software. SSMED experiments were conducted for various conditions and layer-depositioning quality was investigated.

2.5 Metallographic and mechanical tests

A comprehensive microstructure study was conducted for each stage. Microstructure of thixo-extruded and depositioned layers, their bonding and interface were studied. Alloys of Sn-Pb are difficult metallographic subjects; hence, after sandpaper grinding, the metallographic specimens were electro-polished and electro-etched by using a 24-V power supply and electrolyte containing 6% perchloric acid, 14% distilled water, and 80% ethanol for 60 s.

The samples were analyzed with Olympus BH2 UMA optical microscope and SEM was performed with a TEScan Vega3 XMU Scanning Electron Microscope equipped with an EDAX energy dispersive X-ray analyzer (EDS) at 20 keV accelerating voltage. Then average grain size and shape factor (morphology) were measured using Fiji image analyzing software. A measure of globularity of the structure can be achieved by determining the shape factor [35]. Shape factor between 0.6 and 1 is desirable for thixo-forming processes [36].

3D printed simple parts are shown in Fig. 4. To evaluate printing and layers joint quality, a number of mechanical tests were carried out on the SSMED parts. Sub-sized tensile and Vickers micro hardness tests were performed besides studying the fracture appearance of the tensile sample. Tensile test samples were obtained from longitudinal depositioning on the X-Y plane.

3 Rheological model and properties

3.1 Thixotropic model

The most important parameter in SSMs that influence almost all of the rheological properties of the slurry is the percentage

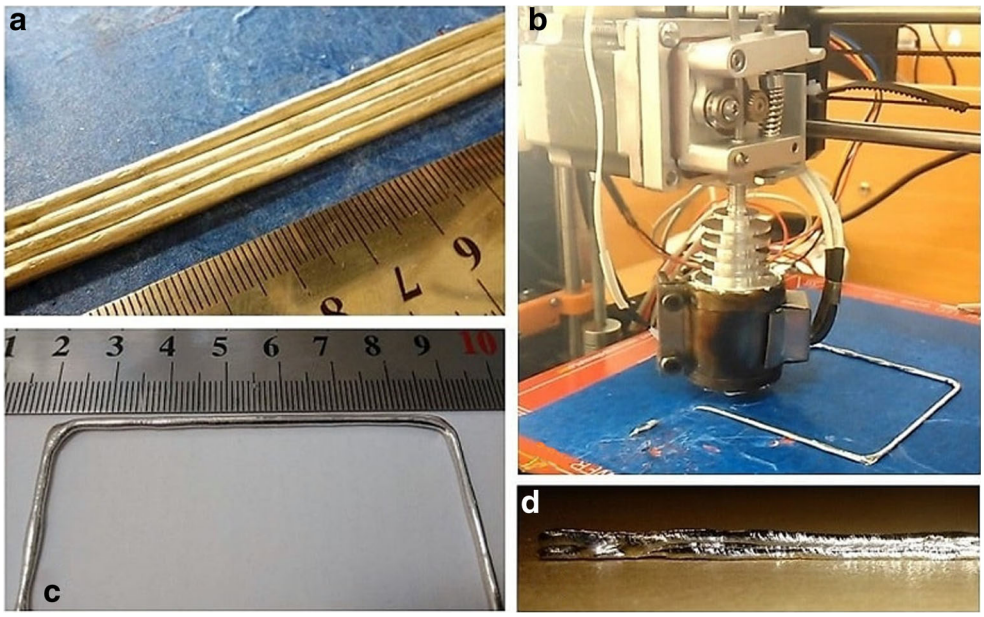

Fig. 4 Deposited layers of semi-solid alloy. **a** Four layers printed adjacent to each other. **b** Thixo-extruder printing a sample. **c** A printed single layer square shape. **d** A three layers printed sample

of solid fraction, f_s [37]. For both of the studied alloys, the corresponding solid fractions at the test temperatures were calculated from the Scheil equation [38]:

$$C_s = k\, C_0\, (1-f_s)^{k-1} \tag{2}$$

where C_s is the concentration of solute in the solid, at a fractional distance along the bar, f_s, C_0 is the initial concentration of the liquid, and k is the partition coefficient C_s/C_l. Using this relation and the phase diagram of Sn-Pb alloy, the solid fraction of alloys was obtained at different temperatures in the semi-solid state.

Thixotropy indicates the time taken to move from one state of microstructure to another and return back [39]. The microstructural driving force arises from the competition between breakdown due to flow stresses and the buildup due to in-flow collisions and Brownian motion [39].

Then thixotropy is usually introduced via the time derivative of the structure parameter, $d\lambda/dt$, which is given by the sum of the buildup and breakdown terms. These are only controlled by the shear rate and the current level of structure λ [40]. A mathematical model that describes comprehensively all aspects of the thixotropic rheology is extremely difficult to develop [41, 42]. However, it is known empirically that shear-thinned materials take much longer times to buildup than thixo-extrusion-produced materials [43, 44]. To explain the rheological model used, the constitutive equation for thixotropy could be expressed as follows [40]:

$$d\lambda \Big/ dt = a(1-x\lambda) - b\lambda \dot{\gamma}^{m} \tag{3}$$

where a, b, γ, and m are buildup constant, breakdown constant, shear rate, and power index, respectively. When $x = 1$, this is the cross steady state equation that gives the equilibrium viscosity [45]:

$$\eta_e = \eta_\infty + \frac{\eta_o - \eta_\infty}{1 + k\dot{\gamma}^{m}} \tag{4}$$

The buildup rate is constant, while breakdown can be constant or be made to depend linearly on the shear rate [45]. For the investigated alloys, the rheological properties and apparent viscosity in each test condition were derived from cross equation in which Sn-Pb alloys with solid fractions of 0.35 to 0.5 fit well [33]. So the cross model was used for the calculation of alloys apparent viscosity at different thixo-extrusion test conditions.

3.2 Liquefier dynamics

There exist some assumptions that are admissible for thixo-extrusion dynamics such as the melt incompressibility, a no-slip boundary condition at the chamber's walls, and a fully developed, steady-state, and laminar flow. To account for the material being solid at the entry of the thixo-extruder, the plug flow is assumed at the channel entry. Therefore, the fraction of the feeder force to cross-section of the filament implies the pressure difference Δp needed to flow through the channel and the nozzle [46]. Here, just like capillary rheometer, it follows [47]:

$$\eta = \frac{\Delta p}{2\dot{\gamma}_w \left[\left(L \Big/ R \right) + e \right]} \tag{5}$$

If $L/R < 50$, the Bagley correction is necessary for considering end effects [47]: $e = \Delta p/2\tau_w$

From Hagen–Poiseuille law for laminar flow through a pipe of circular cross-section, volumetric flow rate is as follows:

$$Q = \frac{\pi R^4 \Delta p}{8\eta L} \tag{6}$$

Up to now, only power-law viscosity models have been used in published studies of polymeric FDM liquefiers [19]. However, more complicated rheological behavior of SSMs in the thixo-extruder is needed to be considered. Shear rates in the nozzle of FDM machines are commonly in the range of 100–200 per second, but in the present study, due to larger nozzle size, it is slightly lower than these values. Shear rate drives are computed from the following equation for a fully developed laminar flow [48]:

$$\dot{\gamma}_w = \dot{\gamma}_a * \left(\frac{3}{4} + \frac{1}{4} \frac{\partial(\ln Q)}{\partial(\ln \tau_w)} \right) = \frac{8V}{D} \left(\frac{3n+1}{4n} \right) \tag{7}$$

where $(3n + 1)/4n$ is the Rabinowitsch correction coefficient and, for the case of common shear-thinning materials, becomes 1.375 [47].

Another estimate for extrudability of a filament in FDM process is given by the following equation [3] that ensures viscosities lower than 20 kPa.s are applicable for the investigated semi-solid alloys.

$$\frac{E}{\eta} \geq \frac{8Q\left(L \Big/ R\right)^2}{\pi^3 r^4 k} \tag{8}$$

L/R is the slenderness ratio of the filament and k is the scaling factor (experimentally determined). Four recent equations have been the basis for the thixo-extruder design.

Fortunately, the small size of filament allows nearly uniform temperature in the melt to be achieved quickly with variations of often less than 0.5 °C through the wall to centerline. In the examination range for the solid fraction in SSMED, which was 0.3–0.4, the sensitivity of f_s to temperature was about 6 °C per 10% changes in solid fractions. This meant having ± 1 °C fluctuations in temperature resulting up

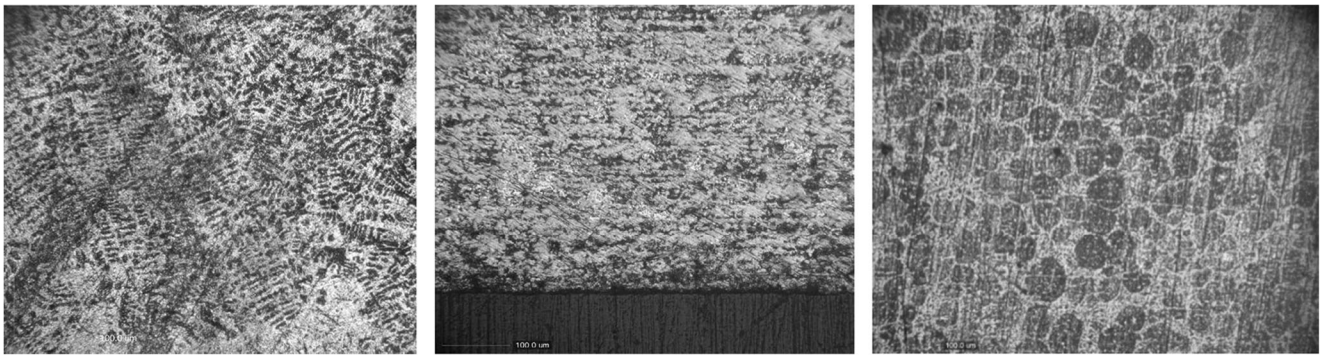

Fig. 5 OM microstructure of the alloy before (left) and after room temperature extrusion (middle) and SIMA processed wire (right)

to 0.05 variations in solid fractions, and hence, good controllability of the microstructure was possible.

In addition, comparison of exiting bead width and nozzle diameter revealed that the presence of solid globules in the slurry exiting from the nozzle results in low die swelling in comparison with fully melted alloys or materials that do not have some solid particles in their medium [41].

4 Results and discussion

Metallurgical studies on the specimens after each stage reveal a fair understanding of the microstructural evolutions during the printing process. The photomicrographs of the Pb-40Sn alloy before and after room temperature extrusion confirm successful generation of directional fine-grained microstructure. This microstructure is very suitable to form globular construction when exposed to semi-solid temperature [49]. The isothermal holding of the produced wires in an oven and then going through water quenching promptly gave the desired microstructure of SSMED feedstock. Figure 5 depicts these microstructure evolutions. Finally, when the globular wire was reheated in thixo-extruder and deposited on the lower surface, minimum microstructural changes occurred in fabricated part (Fig. 6). However, the interlayer adhesion and the interface microstructure have significant effects on the mechanical properties of the final product.

In a good metallurgical joint, there is no sharp microstructural transition at the interface and this was achieved in SSMED process too, so that it is difficult to recognize layers' interface in most of the studied interfaces. Looking at the middle of Fig. 7, it could be seen that there are no visible interface between the two layers indicating a suitable printing of the layers. Back scattered and SEM micrographs of one area at the ending of two successive layers were represented in the figure alongside. Both sides of the interface between two deposited beads have a maximum admissible solid fraction. In the case of Sn-Pb, this solid fraction limit is

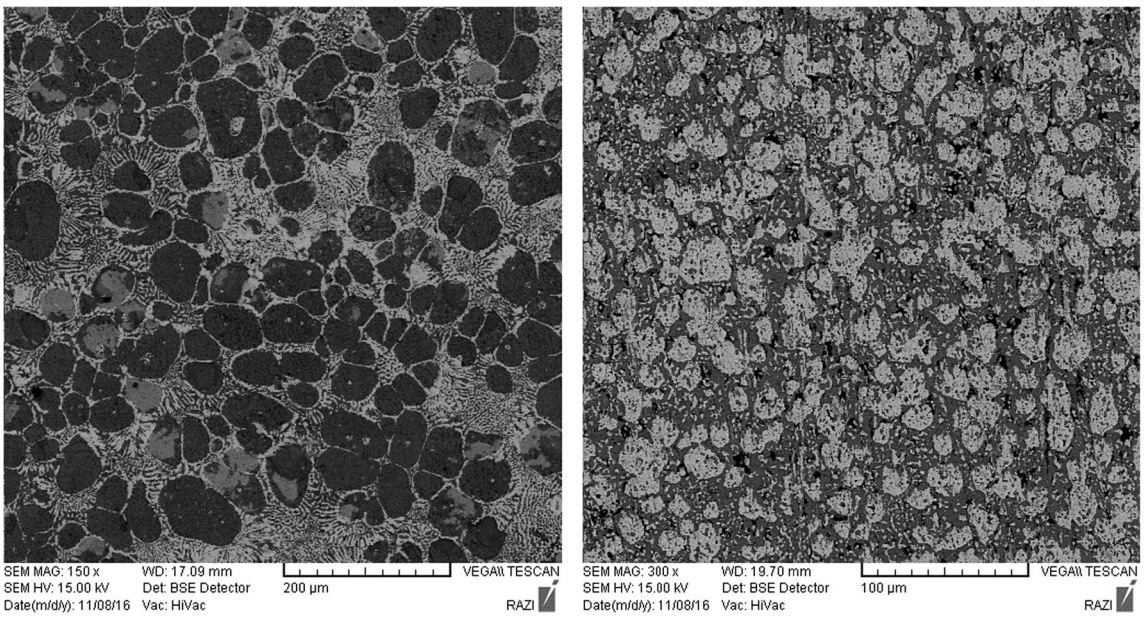

Fig. 6 BSE microstructure of deposited layers for investigated alloys, Sn-15Pb (left), and Pb-40Sn (right)

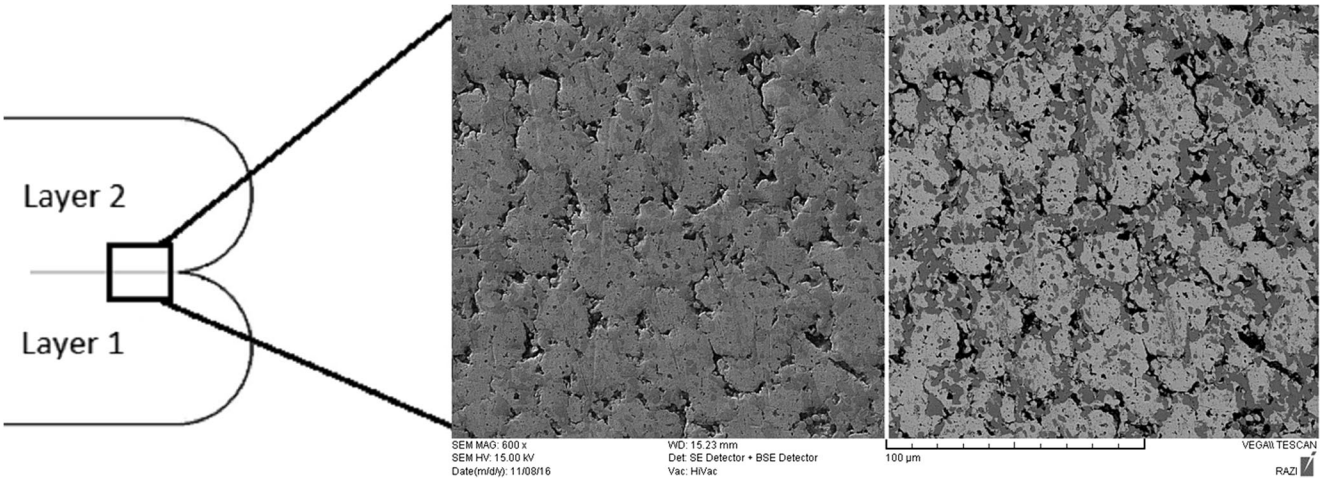

Fig. 7 SEM and BSE of the interface between two deposited layers

approximately 15% [50]. This is due to unique properties of SSMs and high diffusivity of the liquid phase alongside the solid particles [51]. Favorable microstructure dimensions for SSM processes are grain sizes smaller than 100 μm and shape factors more than 0.6 [49]. In this study, the resulted microstructure of SSMED process has typically finer globular grains with average shape factor of 0.7, which indicates a desirable microstructure.

Choosing the optimum shear rates and solid fractions for the thixo-extrusion tests, segregation of solid particles did not occur. Figure 8 demonstrates the X-ray diffraction (EDS) result of the surface of a thixo-extruded layer, from which it could be seen that the chemical composition of the exiting slurry hardly changed by time. EDS analysis was performed to ensure the success of the thixo-extruding process and the absence of phase segregation phenomena. The results indicated that, for the thixo-extruding condition, the material was uniformly discharged from the nozzle without any problem of liquid leakage, and the layers were deposited with near nominal composition.

Also because of the process low operational temperatures, shape changes due to thermal gradients within the part are minimized. Using larger nozzle diameter and lower solid fraction, higher deposition rates could be achieved as far as the flow remains controllable. This method allows high deposition rates of currently up to 0.8 kg/h.

In the micro hardness tests, the results show that hardness values in the layers' interface differ by 4% from those within the inner layer. Figure 9 shows the hardness values for the seven positions from the middle of one layer to another. The mechanical properties of the printed parts are also presented in Table 2 in comparison with the cast alloys. The results show that tensile strength of the SSMED parts in the direction of printing is higher than the cast alloys.

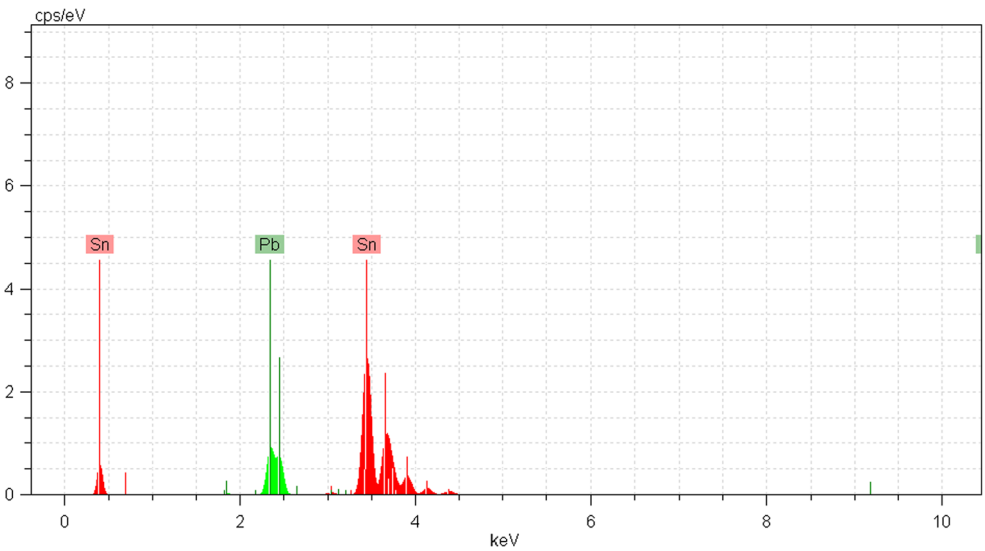

Fig. 8 EDS analysis of the surface of a thixo-extruded layer (81–19 wt% Sn-Pb)

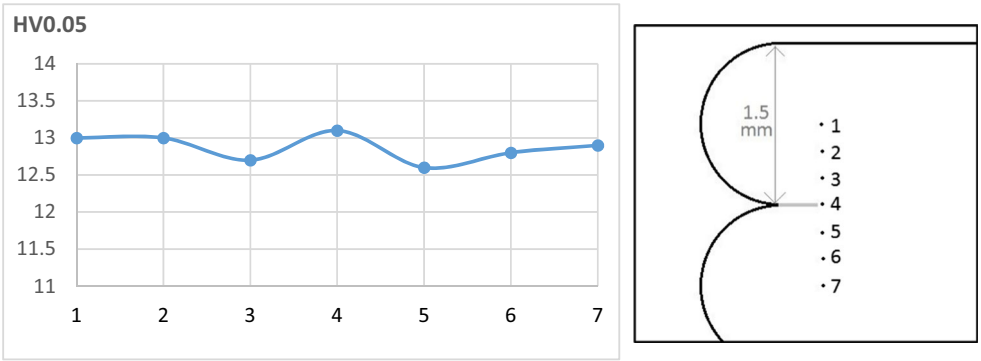

Fig. 9 Distribution of hardness in the successive layers

5 Conclusion

This paper presents a method of metal AM by semi-solid metal extrusion and deposition, SSMED, route. The main concern of the paper was to introduce a new method using semi-solid metallic slurries in extrusion-based AM. Fine control on temperature gave this opportunity to deposit metals just like toothpaste. This was due to special rheological properties of SSMs. This paper presented a pilot study on thixo-extruding a wire to make a continuous bead of semi-solid metal that could be depositioned layer by layer to build a metallic part in three dimensions. According to the results, it is concluded that preconditioned metallic filaments could be deposited successfully on a substrate in a semi-solid state. This process was successfully implemented on a model alloy and illustrated the possibility of using semi-solids for AM, and overcomes the challenges of joining successive semi-solid layers. This research has clearly shown that the SSMED parts made of low-temperature Sn-Pb alloys have good mechanical properties and controlled microstructure.

This new method has its own advantages and disadvantages. Lower operational temperatures in comparison with currently available metal AM techniques resulted in lower energy consumption and lower thermal shrinkage. From metallurgical point of view, all of the commercial metal AM technologies have a number of drawbacks; the most important being the existence of porosity or undesirable grains due to high temperature gradients. In the case of SSMED, almost none of these limitations exist and the microstructure of the whole part is comparable to die cast components. On the other hand, more control on continuous thixo-extruding process and implementing finer nozzle will increase the precision and capabilities of this method.

The findings in this work suggest that this approach makes it conceivable to develop SSMED to other industrial alloys. This process has the potential to apply to higher melting temperature alloys such as aluminum alloys, titanium alloys, steels, and super alloys.

Table 2 Mechanical properties of the printed parts (average values of three or more tests results)

Material		UTS (MPa)	Hardness (HV0.05)
Sn-15Pb	SSMED part	43.8	14.4
	Casted part	41.2	11.2
Pb-40Sn	SSMED part	37.1	12.8
	Casted part	35.3	9.5

References

1. Huang SH, Liu P, Mokasdar A, Hou L (2012) Additive manufacturing and its societal impact: a literature review. Int J Adv Manuf Technol 67(5–8):1191–1203. https://doi.org/10.1007/s00170-012-4558-5
2. Thompson MK, Moroni G, Vaneker T, Fadel G, Campbell RI, Gibson I, Bernard A, Schulz J, Graf P, Ahuja B (2016) Design for additive manufacturing: trends, opportunities, considerations, and constraints. CIRP Ann Manuf Technol 65(2):737–760
3. Bikas H, Stavropoulos P, Chryssolouris G (2016) Additive manufacturing methods and modelling approaches: a critical review. Int J Adv Manuf Technol 83(1–4):389–405
4. Guo N, Leu MC (2013) Additive manufacturing: technology, applications and research needs. Front Mech Eng 8(3):215–243. https://doi.org/10.1007/s11465-013-0248-8
5. Eckel ZC, Zhou C, Martin JH, Jacobsen AJ, Carter WB, Schaedler TA (2016) Additive manufacturing of polymer-derived ceramics. Science 351(6268):58–62
6. Frazier WE (2014) Metal additive manufacturing: a review. J Mater Eng Perform 23(6):1917–1928. https://doi.org/10.1007/s11665-014-0958-z
7. Deckers J, Vleugels J, Kruth JP (2014) Additive manufacturing of ceramics: a review. J Ceram Sci Technol 5(4):245–260
8. Herzog D, Seyda V, Wycisk E, Emmelmann C (2016) Additive manufacturing of metals. Acta Mater 117:371–392
9. Sing SL, An J, Yeong WY, Wiria FE (2016) Laser and electron-beam powder-bed additive manufacturing of metallic implants: a review on processes, materials and designs. J Orthop Res 34(3):369–385. https://doi.org/10.1002/jor.23075
10. Williams CB, Cochran JK, Rosen DW (2011) Additive manufacturing of metallic cellular materials via three-dimensional printing. Int J Adv Manuf Technol 53(1–4):231–239

11. Baufeld B, Brandl E, Van der Biest O (2011) Wire based additive layer manufacturing: comparison of microstructure and mechanical properties of Ti–6Al–4V components fabricated by laser-beam deposition and shaped metal deposition. J Mater Process Technol 211(6):1146–1158
12. Ding D, Pan Z, Cuiuri D, Li H (2015) Wire-feed additive manufacturing of metal components: technologies, developments and future interests. Int J Adv Manuf Technol 81(1–4):465–481
13. Alberti EA, da Silva LJ, D'Oliveira ASC (2016) Additive manufacturing: the role of welding in this window of opportunity. Weld Int 30(6):413–422
14. Brandl E, Baufeld B, Leyens C, Gault R (2010) Additive manufactured Ti-6Al-4V using welding wire: comparison of laser and arc beam deposition and evaluation with respect to aerospace material specifications. Phys Procedia 5:595–606
15. Clark D, Bache M, Whittaker M (2008) Shaped metal deposition of a nickel alloy for aero engine applications. J Mater Process Technol 203(1):439–448
16. Pouyafar V, Sadough S, Hosseini F, Jabbari A (2013) High temperature flow behaviour of semi-solid steel alloys. In: Solid state phenomena. Trans Tech Publ, pp 365–369
17. Gao W, Zhang Y, Ramanujan D, Ramani K, Chen Y, Williams CB, Wang CCL, Shin YC, Zhang S, Zavattieri PD (2015) The status, challenges, and future of additive manufacturing in engineering. Comput Aided Des 69:65–89. https://doi.org/10.1016/j.cad.2015.04.001
18. Rice CS, Mendez PF, Brown SB (2000) Metal solid freeform fabrication using semi-solid slurries. JOM 52(12):31–33. https://doi.org/10.1007/s11837-000-0065-5
19. Turner BN, Strong R, Gold SA (2014) A review of melt extrusion additive manufacturing processes: I. Process design and modeling. Rapid Prototyp J 20(3):192–204
20. Fan Z (2002) Semisolid metal processing. Int Mater Rev 47(2):49–85
21. Rice CS (1995) Solid freeform fabrication using semi-solid processing. Doctoral dissertation, Massachusetts Institute of Technology, Doctoral dissertation
22. Kirkwood D (1994) Semisolid metal processing. Int Mater Rev 39(5):173–189
23. Mireles J, Espalin D, Roberson D, Zinniel B, Medina F, Wicker R (2012) Fused deposition modeling of metals. In: International SFF symposium held in Austin, Texas. pp 6–8
24. Finke S, Feenstra F (2002) Solid freeform fabrication by extrusion and deposition of semi-solid alloys. J Mater Sci 37(15):3101–3106
25. Cao W, Miyamoto Y (2006) Freeform fabrication of aluminum parts by direct deposition of molten aluminum. J Mater Process Technol 173(2):209–212
26. Orme M, Liu Q, Smith R (2000) Molten aluminum micro-droplet formation and deposition for advanced manufacturing applications. Aluminum Trans 3(1):95–103
27. Turng L, Wang K (1991) Rheological behaviour and modelling of semi-solid Sn-15% Pb alloy. J Mater Sci 26(8):2173–2183
28. Lashkari O, Ghomashchi R (2007) The implication of rheology in semi-solid metal processes: an overview. J Mater Process Technol 182(1):229–240
29. Mohammed M, Omar MZ, Salleh M, Alhawari K, Kapranos P (2013) Semisolid metal processing techniques for nondendritic feedstock production. Sci World J 2013. doi:https://doi.org/10.1155/2013/752175
30. Atkinson HV (2013) Alloys for semi-solid processing. In: Solid state phenomena. Trans Tech Publ, pp 16–27
31. Laplume A, Anzalone GC, Pearce JM (2015) Open-source, self-replicating 3-D printer factory for small-business manufacturing. Int J Adv Manuf Technol 85(1–4):633–642. https://doi.org/10.1007/s00170-015-7970-9
32. Venkataraman N, Rangarajan S, Matthewson M, Harper B, Safari A, Danforth S, Wu G, Langrana N, Guceri S, Yardimci A (2000) Feedstock material property-process relationships in fused deposition of ceramics (FDC). Rapid Prototyp J 6(4):244–253
33. Liu T, Ward P, Atkinson HV, Kirkwood D (2003) Response of semi-solid Sn-15 pct Pb to rapid shear-rate changes. Metall Mater Trans A 34(2):409–417
34. Bellini A, Guceri S, Bertoldi M (2004) Liquefier dynamics in fused deposition. J Manuf Sci Eng 126(2):237–246
35. Pouyafar V, Sadough S, Hosseini F, Jabbari A (2013) The influence of reheating profile on the final microstructure of the semi-solid S600 and K100 tool steels. In: Solid state phenomena. Trans Tech Publ, pp 204–208
36. Hirt G, Kopp R (2009) Thixoforming. John Wiley & Sons
37. Flemings M (2013) Semi-solid forming: the process and the path forward. Metall Sci Technol 18(2):2
38. Zhang D (2015) Thermodynamic characterisation of semi-solid processability in alloys based on AL-SI, AL-CU and AL-MG binary systems. Department of Engineering, Doctoral dissertation
39. Barnes HA (1997) Thixotropy—a review. J Non-Newtonian Fluid Mech 70(1):1–33
40. Kirkwood DH, Ward PJ (2004) Numerical modeling of semisolid flow under processing conditions. Steel Res Int 75(8/9):519–524
41. Barkhudarov M, Bronisz C, Hirt C (1996) Three-dimensional thixotropic flow model. In: 4th International Conference on Semi-Solid Processing of Alloys and Composites. pp 110–114
42. Charreyron PO, Flemings MC (1985) Rheology of semi-solid dendritic Sn-Pb alloys at low strain rates: application to forming process. Int J Mech Sci 27(11):781–791
43. Jabbari A, Sadough SA, Pouyafar V (2014) Rotational rheology of A356 semi-solid alloy at low solid fractions. Adv Mater Res 1019:74–80
44. Corvisier P, Nouar C, Devienne R, Lebouché M (2001) Development of a thixotropic fluid flow in a pipe. Exp Fluids 31(5):579–587
45. Atkinson HV (2005) Modelling the semisolid processing of metallic alloys. Prog Mater Sci 50(3):341–412
46. Turner BN, Gold SA (2015) A review of melt extrusion additive manufacturing processes: II. Materials, dimensional accuracy, and surface roughness. Rapid Prototyp J 21(3):250–261. https://doi.org/10.1108/rpj-02-2013-0017
47. Vlachopoulos J, Strutt D (2003) The role of rheology in polymer extrusion. In: New technology for extrusion conference. Milan. pp 20–21
48. Finke S, Wei W, Feenstra F (1999) Extrusion and deposition of semi-solid metals. In: Proc solid freeform fabrication symposium, Austin, TX. pp 9–11
49. Hassas-Irani S, Zarei-Hanzaki A, Bazaz B, Roostaei AA (2013) Microstructure evolution and semi-solid deformation behavior of an A356 aluminum alloy processed by strain induced melt activated method. Mater Des 46:579–587
50. Mendez P, Rice C, Brown S (2003) Comments on "solid freeform fabrication by extrusion and deposition of semi-solid alloys". J Mater Sci Lett 22(14):1047–1049. https://doi.org/10.1023/a:1024710013774
51. Tzimas E, Zavaliangos A (2000) Evolution of near-equiaxed microstructure in the semisolid state. Mater Sci Eng A 289(1):228–240